Identifying the Lowest Electronic States of the Chlorophylls in the CP47 Core Antenna Protein of Photosystem II†

Frank L. de Weerd,* Miguel A. Palacios, Elena G. Andrizhiyevskaya, Jan P. Dekker, and Rienk van Grondelle

Faculty of Sciences, Division of Physics and Astronomy, Department of Biophysics and Physics of Complex Systems, Vrije Universiteit, De Boelelaan 1081, 1081 HV Amsterdam, The Netherlands

Received May 28, 2002; Revised Manuscript Received September 5, 2002

ABSTRACT: CP47 is a pigment−protein complex in the core of photosystem II that tranfers excitation energy to the reaction center. Here we report on a spectroscopic investigation of the isolated CP47 complex. By deconvoluting the 77 K absorption and linear dichroism, red-most states at 683 and 690 nm have been identified with oscillator strengths corresponding to ∼3 and ∼1 chlorophyll, respectively. Both states contribute to the 4 K emission, and the Stark spectrum shows that they have a large value for the difference polarizability between their ground and excited states. From site-selective polarized triplet-minus-singlet spectra, an excitonic origin for the 683 nm state was found. The red shift of the 690 nm state is most probably due to strong hydrogen bonding to a protein ligand, as follows from the position of the stretch frequency of the chlorophyll 13^1 keto group (1633 cm^{-1}) in the fluorescence line narrowing spectrum at 4 K upon red-most excitation. We discuss how the 683 and 690 nm states may be linked to specific chlorophylls in the crystal structure [Zouni, A., Witt, H.-T., Kern, J., Fromme, P., Krauss, N., Saenger, W., and Orth, P. (2001) *Nature 409*, 739−743].

In oxygenic photosynthesis, two photosystems work in series. Both harvest sunlight, and the excitation energy in each photosystem is transferred to a photochemical reaction center (RC)[1] where a charge separation is initiated (*1*, *2*). In photosystem II (PSII), the released electrons are transferred to plastoquinone, and via the cytochrome b_6f complex to plastocyanin (or cytochrome c_6 in certain cyanobacteria). The redox potential of the oxidized primary electron donor ($P680^+$) is sufficiently high to oxidize water to molecular oxygen. The protons liberated during this process contribute to the transmembrane pH gradient, which provides the driving force for ATP synthesis (*3*).

In PSII, the reaction center (RC) is surrounded by two pigment−protein complexes, the core antennas CP43 and CP47. Their function is to transfer excitation energy from the peripheral light-harvesting complexes to the RC. Only one Chl, located in CP47, absorbs at significantly longer wavelength (690 nm) than that of the primary electron donor P680. Linear dichroism (LD) experiments at 4 K (*4*) indicated that unlike most other Q_y transitions this 690 nm state is oriented perpendicular to the plane of the membrane. The F-695 fluorescence of PSII cores at 77 K originates from the red part of this inhomogeneously broadened band (*5*).

The crystal structure of the PSII core complex of *Synechococcus elongatus* was published recently at a resolution of 3.8 Å (*6*). Six chlorins (four Chls and two pheophytin *a* molecules) constitute the RC, while 28 Chls have been identified as antenna components, of which 14 are bound to CP47, 12 to CP43, and 2 to the D1/D2 complex. Further analysis of the same X-ray data indicated the presence of three additional Chls, of which two are bound to CP47 (*7*), bringing its Chl content to 16. One of these additional Chls is in the vicinity of His-114, which was suggested to be the prime candidate to bind the 690 nm pigment (*8*).

Because of the PSII structures that have been published recently (*6*, *9*) and the forecast of a structure at higher resolution, establishing the relation between the structure and spectroscopy of the PSII core has become a major topic of investigation. In this study we focus our attention on the CP47 part of the complex.

Recently, we showed that the major steps of excitation energy transfer upon excitation at 660, 670, and 677 nm occur in this complex in 0.2 and 2 ps at 77 K, thereby populating red-shifted states at 683 nm, followed by an additional energy transfer step of ∼17 ps to the 690 nm state (*10*). Red states at ∼683 and 690 nm are also present in a hole-burning study by Chang et al. (*11*): a 684 nm state was identified that transfers its energy 'downhill' in ∼10 ps. In our analysis, it was found that not all of the 683 nm states transfer energy to the 690 nm pigment. Furthermore, it was argued that the red shift of the 683 nm band can be explained by excitonic interactions calculated from the structure, but that for the 690 nm state a specific 'red' site energy is required (*10*). In contrast, Chang et al. (*11*) proposed that the 690 nm state is part of a weakly coupled dimer, with the higher exciton component at 687 nm that was identified in persistent nonphotochemical hole-burning

† This research was supported by The Netherlands Organization for Scientific Research (NWO) via the Dutch Foundations for Earth and Life Sciences (A.L.W.).

* Corresponding author. Tel.: (+31) 20 4447934. Fax: (+31) 20 4447999. E-mail: weerd@nat.vu.nl.

[1] Abbreviations: Chl, chlorophyll *a*; fwhm, full width at half-maximum; FLN, fluorescence line narrowing; LD, linear dichroism; CD, circular dichroism; OD, optical density; PS, photosystem; T−S, triplet-minus-singlet.

10.1021/bi0261948 CCC: $22.00
Published on Web 11/22/2002

(NPHB) spectroscopy. In population bottleneck hole-burning or triplet-minus-singlet (T−S) spectroscopy, this 687 nm state was not observed due to its believed very short lifetime (*11*). Nonselectively excited time-resolved T−S spectra at 4 K also revealed the presence of two spectrally different species (peaking at 684 and 686 nm) with different triplet state lifetimes (*12*).

Here, we report the results of a variety of spectroscopic experiments on the CP47 complex. In particular we focus on the spectroscopic properties of the lowest states (i.e., absorbing in the region 680−690 nm), with the aim to explain their red shifts and the energy transfer that takes place between them. We deconvolute the CP47 absorption and LD spectra at 77 K in a set of common spectral components. We present polarized site-selective T−S spectra, yielding information on the orientations of the states bleached by the triplet formation. Furthermore, we present polarized emission and fluorescence line narrowing (FLN) experiments performed at 4 K, yielding information on the amount of energy transfer and nature of the fluorescent state(s) at 4 K. The pigment pools in CP47 are further characterized by measuring the 77 K Stark spectrum. The spectroscopic properties of the Chls are intimately related to energy transfer. Characterizing these properties therefore helps in getting a better understanding of the function of CP47.

MATERIALS & METHODS

Sample Preparation. CP47−RC and CP47 complexes were purified from spinach as described elsewhere (*12*, *13*). The complexes were dissolved in a buffer such that the final sample contained 0.09% (w/v) β-DM, 20 mM NaCl, 65% (v/v) glycerol, and 20 mM BisTris (pH 6.5). For the Stark experiments, these concentrations are 0.12% (w/v) β-DM and <10 mM NaCl. For the linear dichroism (LD) experiments, 6.4% (w/v) gelatine was added to the buffer (*14*).

Linear Dichroism. Linear dichroism (LD) is the differential absorption of two orthogonal linearly polarized light beams in a macroscopically oriented sample. The LD spectra were recorded on a home-built setup (*15*). The sample was diluted in the molten gel (at ∼32 °C) to an optical density (OD) of ∼0.5 cm^{-1} in the Q_y maximum (77 K). The simultaneously recorded absorption spectrum was not affected by the gel and the exposure to elevated temperatures. The 12.5 × 12.5 mm polymerized gel was oriented by squeezing in two perpendicular directions to the 10 × 10 mm dimensions of the cuvette.

Fluorescence Line Narrowing. Site-selective emission spectra were recorded as described elsewhere (*16*). In short, a CW dye laser (Coherent CR599) with DCM dye and a bandwidth of ∼0.1 nm, pumped by an Ar^+ laser (Coherent Innova 310), was used for excitation. The power was attenuated to ∼100 $\mu W/cm^2$, to minimize the effects of hole-burning. Emission spectra were detected with a 0.5 m spectrograph (Chromex 500IS) and a CCD camera (Chromex Chromcam 1) with 0.25 nm resolution. Parallel (VV), magic angle, and perpendicular (VH) polarized spectra were measured by rotating a polarizer behind the sample relative to a polarizer in front of the sample. All the spectra were corrected for the sensitivity of our detection system by comparison of a measured spectrum emitted by a Tungsten halogen lamp with the spectrum provided by the lamp manufacturer. The anisotropy of the emission was calculated according to

$$r(\lambda) = \frac{F_{VV}(\lambda) - F_{VH}(\lambda)}{F_{VV}(\lambda) + 2F_{VH}(\lambda)} \quad (1)$$

Site-Selective Absorbance Difference Spectroscopy. Reversible light-induced absorption difference spectra, also known as light-induced triplet-minus-singlet (T−S) absorption difference spectra, or transient hole-burning spectra with the triplet state acting as a population bottleneck, were recorded as described by Kwa et al. (*17*). In short, the same laser source was used as for the FLN experiment, while the excitation powers were increased to 100 mW/cm^2 to create a steady-state Chl triplet population during illumination. Probe (halogen lamp in combination with a monochromator) and excitation beams were at right angles. The absorbance-difference spectra were measured with double lock-in detection. The detection-wavelength independent contribution from fluorescence and scattered laser light (measured without probe beam) was subtracted from the spectra.

Stark Spectroscopy. The sample for the Stark experiment was concentrated to an OD of ∼100 cm^{-1}, such that after adding the glycerol buffer the OD was 0.3 over the ∼100 μm between the electrodes. Stark spectra were recorded on a home-built setup (*17*). An electric field of 2.3×10^5 Vcm^{-1} was applied. For randomly oriented samples in a frozen glass, the absorption change induced by an externally applied electrostatic field provides information on the change in dipole moment and polarizability associated to a transition. The first derivative (of the ground-state absorption) contribution to the Stark spectrum reflects the difference polarizability between the ground and excited state ($Tr\Delta\alpha$), whereas a difference in permanent dipole moment between these states ($\Delta\mu$) gives rise to a second derivative contribution to the Stark spectrum (*19*, *20*). Estimates for $Tr\Delta\alpha$ and $\Delta\mu$ were obtained by simultaneously fitting the absorption (with a sum of Gaussian functions) and Stark spectrum (with first and second derivatives of these functions) using a nonlinear least-squares fitting program (*18*, *21*).

RESULTS

Linear Dichroism. Linear dichroism yields information on the orientation of transition dipoles in a particle relative to an axis of orientation. For the PSII core complex, this technique may yield valuable information because at the current resolution of 3.8 Å the orientation of the planes of the heme groups of the Chls is well-established, but the orientation of the individual Q_y and Q_x transitions is basically not known. Linear dichroism has successfully been applied to obtain information on the direction of the transition dipole moments of the Chls in the 3.4 Å structure of LHCII (*22*−*24*).

We recorded the LD spectrum of CP47 at 77 K in a gel based on gelatine. The absorption spectrum (Figure 1, solid line; Q_y region in inset, thick line) exhibits the characteristic CP47 absorption peaking at 674.5 nm, and with a pronounced shoulder at 683 nm. The inverted second derivative spectrum displays maxima at 660, 670, 676, and 683 nm, in agreement with spectra recorded in a glycerol/water glass (*4*, *11*, *17*). Apparently, the 77 K absorption of CP47 is not affected by

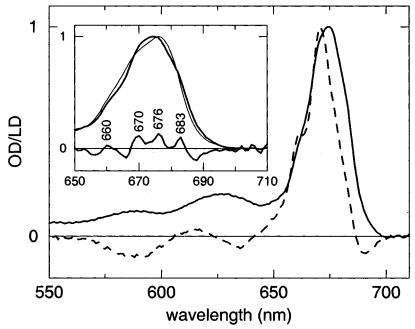

FIGURE 1: Simultaneously recorded absorption (solid line) and LD (dashed line) spectra of CP47 at 77 K, stretched in a gel based on gelatine. Inset shows the same absorption in the Q_y region plus the inverted second derivative of this spectrum (thick solid lines), compared to the absorption in a stretched gel based on polyacrylamide (thin solid line).

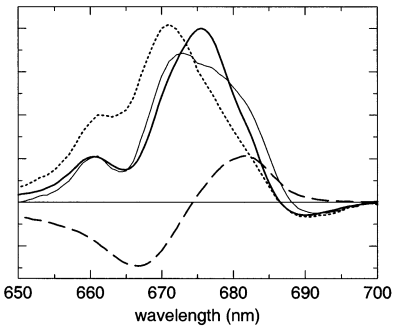

FIGURE 2: Linear dichroism spectra at 77 K of CP47 (dotted line), PSII reaction center (dashed line, taken from ref *25*), and CP47−RC (thick solid line). These three spectra were scaled in such a way that the sum of CP47 and RC (thin solid line) best resembles the CP47−RC spectrum.

the relatively mild conditions required for the formation of a gel based on gelatine. The simultaneously recorded LD spectrum (Figure 1, dashed line) is mainly positive in the Q_y and negative in the Q_x region. The spectrum peaks at 671 nm and is 3.5 nm blue shifted compared to the absorption spectrum. The second derivative of the LD spectrum displays minima at 661, 670.5, 677, and 683 nm (not shown), in close agreement with the second derivative of the absorption spectrum. Furthermore, a negative band at 690 nm is clearly resolved.

Normally, detergent-isolated pigment−protein complexes orient like disc-shaped particles with the plane of the disk parallel to the plane of the membrane. Hence, the orientation axis upon squeezing lies in the (imaginary) membrane plane. For CP47, however, this is uncertain because this protein is relatively small and exhibits a large extrinsic loop. To check the orientation, we measured the LD spectrum of the larger CP47−RC complex (the LD of the PSII reaction center is well-known, see for example refs *25* and *26*). If the CP47 orientation axis lies in the (imaginary) membrane plane, as we can safely assume for the RC and the CP47−RC particles, the CP47 and RC LD should add up to the CP47−RC LD. In Figure 2, the 77 K LD spectra of the CP47 (dotted line), RC (dashed line, taken from ref *25*), and CP47−RC (thick solid line) complexes are displayed. The three spectra have been scaled in such a way that the sum of CP47 and RC LD (thin solid line) best resembles the CP47−RC spectrum. Given the fact that the CP47−RC absorption is not a linear combination of CP47 and RC absorption (see, e.g., ref *27*),

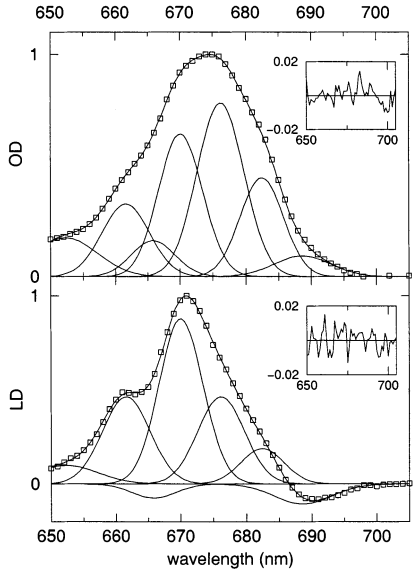

FIGURE 3: A fit of the simultaneously recorded absorption (top) and LD (bottom) spectra of CP47 at 77 K. Data points are indicated by squares. Solid lines indicate a fit on an energy scale of these spectra with Gaussian bands (displayed on a wavelength scale). The positions and widths (fwhm) are the same in both spectra, see Table 1. The insets show the residuals.

the differences between the measured and reconstituted CP47−RC spectra are small, from which we conclude that also the CP47 orientation axis lies more or less in the (imaginary) membrane plane.

Then, in case of orienting the sample by two-dimensional squeezing, positive LD signs indicate an average angle between the Q_y dipoles and the membrane plane smaller than 35°, while negative LD signals indicate an angle larger than 35° (*28*). The results indicate that most of the Q_y transitions (except that of the 690 nm transition) are at angles smaller than 35° with the membrane plane and that most of the Q_x transitions are at angles larger than 35° with the membrane plane. Together, the Q_x and Q_y signs imply a perpendicular orientation to the membrane plane for the majority of the Chl rings. The latter is in line with structural information because all the Chl planes identified in the PSII core crystal structure make an angle to the membrane plane larger than 35° (*6*).

The second derivative positions of the LD and absorption spectra almost coincide. We have therefore deconvoluted these spectra in a set of common spectral components: Figure 3 represents such a combined fit with Gaussian bands. The parameters for position and width of the Gaussians are linked in a global analysis of both spectra, and the obtained parameter values are listed in Table 1, together with the number of Chls contributing to each band, when normalizing the total absorption to 16 Chls (*7*). We also listed the LD, normalized on the absorption of each band.

This fit should be interpreted with care. A unique fit is not found, depending on the starting parameters slightly different results are obtained. Moreover, absorption bands at 77 K might not have Gaussians shapes. This approach is therefore more a means to describe rather than a way to explain the spectra. However, our deconvolution provides further evidence that a 690 nm state with a distinct orientation is the lowest-energy state. In the fit, this state carries an oscillator strength corresponding to 0.8 ± 0.2 Chl, in

Table 1: Values for the Position and Width of Gaussian Bands (on an Energy Scale) in a Combined Fit of the Simultaneously Recorded Absorption and LD Spectra of CP47 at 77 K[a]

pos (nm)	width (cm^{-1})	OD scaled to 16	LD/OD (au)
652.3	271	vibronic	vibronic
661.6	198	2.3	1.2
665.8	180	1.0	−0.5
670.1	177	4.0	1.2
676.2	183	5.2	0.5
682.5	167	2.8	0.4
688.9	217	0.8	−1.0

[a] Also listed the absorption of each band (normalized on a total absorption corresponding to 16 Chls) and the LD of each band (normalized on the absorption). Vibronic implies transitions to higher vibronic substates of the Q_y electronic state. See also Figure 3.

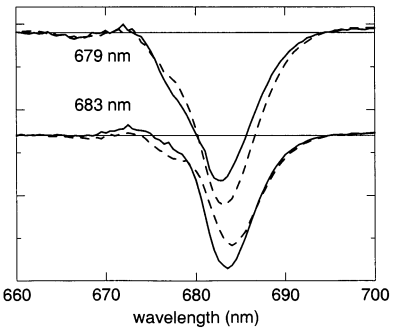

FIGURE 4: Site-selective polarized triplet-minus-singlet absorbance-difference spectra at 4 K recorded with probe light oriented parallelly (solid lines) and perpendicularly (dashed lines) to the laser excitation (679 and 683 nm).

agreement to the assignment of the 690 nm state to a single Chl (*5*). The 683 nm state is oriented at small angles with the plane of the membrane and carries an oscillator strength corresponding to approximately three Chls.

We note that an earlier LD spectrum of CP47 at 4 K, stretched in a gel based on polyacrylamide, also displayed a minimum at ~690 nm, but the maximum (677 nm) was red shifted compared to the absorption (*4*). For an explanation, we first note that the absorption spectrum in the Q_y region of the CP47 complex is affected in such a gel (inset Figure 1, thin line): No shoulder at 683 nm can be discerned, and the absorption maximum is observed at 676 nm. Furthermore, the recorded LD spectrum displays a large amplitude (not shown). We assign these features observed in a gel based on polyacrylamide to denaturation combined with aggregation of the complex: The observed absorption is similar to a 77 K absorption spectrum of CP47 in a buffer without a gel but with a low β-DM concentration (0.03% w/v). Also aggregation of LHCII has been shown to lead to increased and red-shifted LD signals (*29*).

Site-Selective Absorbance Difference Spectroscopy. The Chl excited state can decay to a triplet state via intersystem crossing. The CP47 nonselectively excited time-resolved triplet-minus-singlet (T−S) spectrum at 4 K peaks at 685 nm. The decay associated spectra (DAS) reveal the presence of two spectral species peaking at 684 and 686 nm, with lifetimes of 2.0 and 0.6 ms, respectively (*12*). The contribution of the 684 nm species is half that of the 686 nm species. Carotenoid triplets (after Chl excitation) were only observed on a microsecond time scale. It was concluded that half of the triplets created on Chls (total yield of initial triplet formation at 4 K is ~0.3) are transferred to β-carotene (on a submicrosecond time scale), whereas the other half is apparently not in contact with either of the two β-carotenes and gives rise to the millisecond lifetimes of the Chl triplets. To explain these observations, it was suggested that a special pathway of triplet transfer to β-carotene from red Chls (the 690 nm pigment?) exists (*12*).

To further shed light on these observations, we have studied the triplet formation in a different manner. A narrow-bandwidth laser with vertical polarization and sufficient excitation power (100 mW/cm^2) creates a population of Chl triplet states. The T−S spectra are recorded by a second light source using lock-in detection. This is done with probe light parallel and perpendicular to the laser light, yielding information on the orientations of the states bleached by the triplet formation. Kwa et al. (*30*) applied this technique to study the PSII RC complex.

Figure 4 shows the parallel (solid lines) and perpendicular (dashed lines) spectra upon excitation at 679 and 683 nm at 4 K. After 683 nm excitation, the T−S spectra display a main band around ~684 nm due to bleaching of singlet states upon the triplet formation. The positive contribution from triplet−triplet absorption is only small. The main band displays a positive anisotropy, whereas a sideband on the blue side of the main bleaching (665−679 nm) displays a negative anisotropy. After 679 nm excitation, the main bleaching in the T−S spectra is at 683 nm, and displays a negative anisotropy, while the bleaching around the excitation wavelength displays a positive anisotropy. The observation of bleaching at 683 nm and bleaching more to the blue with opposite anisotropy signs is a strong indication that these bands are excitonically coupled. The amplitudes of the T−S spectra upon red excitation (>683 nm) were dropping rapidly from one measurement to the next. Most likely the 690 nm band is absent in these spectra because it is permanently bleached due to the high excitation powers required in such an experiment (ascribed to nonphotochemical hole-burning (NPHB) at red excitation that is not reversible during the course of the experiment, this is also present in our 4 K emission experiments, that are performed with much lower (a factor 10^3) excitation powers). However, the absorption spectrum after the experiment was not noticeably different from the one measured before.

It is interesting to compare the T−S spectra with pump−probe spectra measured earlier on the same CP47 complex (*10*). The main difference, apart from the time scales, is the presence of stimulated emission in the pump−probe data. It is to be expected, however, that the Stokes' shifts of the Chls are small, and therefore that the pump−probe spectra at long delay times (nanoseconds) are comparable with the T−S spectra. The T−S spectra presented here are indeed reminiscent of the pump−probe spectra at a few picosecond time delay (*10*). Both experiments show a narrow band at 682−684 nm with similar width and higher exciton components, which exhibit similar anisotropy characteristics in both experiments. Only, as can be expected because of stimulated emission, the pump−probe spectra are 1−2 nm red shifted compared to the T−S spectra. However, due to the presence of a ~17 ps nonconservative relaxation in the pump−probe spectra, thereby populating the 690 nm state, the pump−probe spectra on a longer time become very different

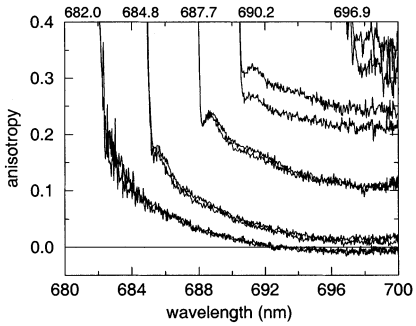

FIGURE 5: Fluorescence anisotropy vs detection wavelength for different excitation wavelengths measured at 4 K. At each excitation wavelength two consecutive measurements were performed; the latter anisotropy values are always smaller due to effects of hole burning.

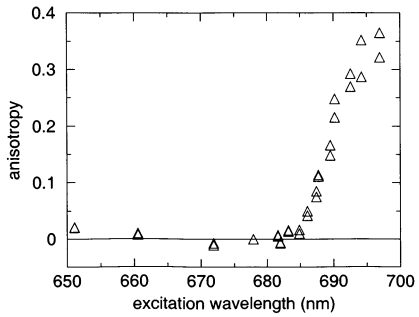

FIGURE 6: Fluorescence anisotropy, averaged between 695 and 700 nm, vs excitation wavelength measured at 4 K. At each excitation wavelength two consecutive measurements were performed; the second anisotropy value is always smaller due to effects of hole burning.

(nonsymmetric and much broader) from the T−S spectra presented here.

Polarized Emission. We have measured the anisotropy of the 4 K emission as a function of the excitation wavelength. Upon nonselective excitation (650 nm) the emission spectrum peaks at 691 nm and has a full width at half-maximum (fwhm) of 12 nm, in agreement with literature spectra (*11*, *12*). This emission exhibits a constant anisotropy close to zero, i.e., due to energy transfer there is no correlation between the angles of the absorbing and emitting dipoles. For various excitation wavelengths within the main emission band, the anisotropy as a function of emission wavelength is plotted in Figure 5. At each excitation wavelength two consecutive measurements were performed; the second anisotropy levels are always lower due to the effects of hole burning (see also the comments about the nonreversible T−S spectra). When exciting into the blue edge of the main emission band (around 683 nm), the anisotropy of the emission just red from the laser wavelength displays an anisotropy of around 0.2. However, the anisotropy in this case is not constant over the emission and drops to zero at the red side of the main emission band. When exciting more to the red, the anisotropy reaches a higher value and becomes less dependent on the emission wavelength. Upon 696.9 nm excitation, the value reaches the theoretical maximum of 0.4, when absorbing and emitting dipoles are oriented parallel (no energy transfer). The observation of a changing anisotropy of the emission over the main emission band upon excitation around 683 nm, versus a constant high value after excitation more to the red is a strong indication that the emission arises from at least two different Chl pools, presumably the 683 and 690 nm states. Although some depolarized "690 nm" emission might contribute to the fluorescence at ∼683 nm after 683 nm excitation, the value of 0.2 indicates that some isoenergetic energy transfer takes place after 683 nm excitation. This implies that at least two electronic states with nonparallel transition dipoles constitute the 683 nm state.

Figure 6 shows the anisotropy of the emission as a function of the excitation wavelength averaged in a region where most of the emission arises from the 690 nm state (between 695 and 700 nm). Some additional excitation wavelengths (compared to Figure 5) are plotted, and the two triangles represent the two consecutive measurements at each excitation wavelength. For excitation wavelengths shorter than 685 nm, the anisotropy value is about zero (the 690 nm state is not excited directly); upon scanning the excitation wavelength to 685 nm and above, the anisotropy rises steeply to a value of ∼0.35 for excitation at about 697 nm.

Fluorescence Line Narrowing. Upon exciting with a narrow-bandwidth laser, FLN is observed when energy transfer does not occur. This is achieved by exciting into the red edge of the absorption spectrum at sufficiently low temperature. The so-obtained line-narrowed spectrum is a probe of the fluorescing Chl and its molecular environment.

Line narrowing at 4 K is observed for excitation wavelengths longer than ∼684 nm. The fluorescence spectrum upon exciting into the red edge of the absorption spectrum (the average of spectra excited at 692.4, 692.8, and 694.4 nm) is shown in Figure 7, plotted as the difference with the excitation wavelength (on a wavenumber scale). A phonon wing (0−200 cm^{-1}), and dozens of vibrational zero-phonon lines up to 1700 cm^{-1}, can be discerned (the electronic zero-phonon line at 0 cm^{-1} is mixed with the Rayleigh scattering of the laser light). The two insets show details of this spectrum. Phonon modes are observed at 20, ∼60, and ∼80 cm^{-1}. When scanning the laser from 692 to 697 nm, the ratio of the 20 cm^{-1} mode over the ∼80 cm^{-1} mode increases (not shown), suggesting a more monomeric behavior of the most red-shifted Chls (see ref *16* for a discussion on the 80 cm^{-1} mode observed in the FLN spectra of the PSII RC complex). The other inset shows the low-energy region of the spectrum. The C═C stretch frequencies of the chlorin ring are observed at 1521 (shoulder), 1534, and 1553 cm^{-1}. These frequencies indicate that most of the emitters are bound to one axial protein ligand (central Mg five-coordinated), whereas the shoulder at 1521 cm^{-1} is a contribution from a Chl with two axial protein ligands (central Mg six-coordinated). In the latter case the C═C stretch frequencies are known to occur ∼10 cm^{-1} lower (*31*, *32*) . The mode observed at 1633 cm^{-1} most likely reflects the 13^1 C═O stretch, suggesting a hydrogen bonding to the protein environment. In the absence of hydrogen bonding, this stretch mode would be observed at 1680−1700 cm^{-1} (*33*). The particular frequency here observed for CP47 (1633 cm^{-1}) is low compared to other subcomplexes of PSII (ranging between 1645 and 1673 cm^{-1} in CP43 (*34*), LHCII (*35*), the reaction center (*16*), and the cyt b_6f complex (*36*)). In Table 2, we have made a list of position and strength (strong/medium/weak) of all vibrational zero-phonon lines observed in CP47, together with the modes observed in CP43 (*34*) and the PSII reaction center (*16*). This list comprises a

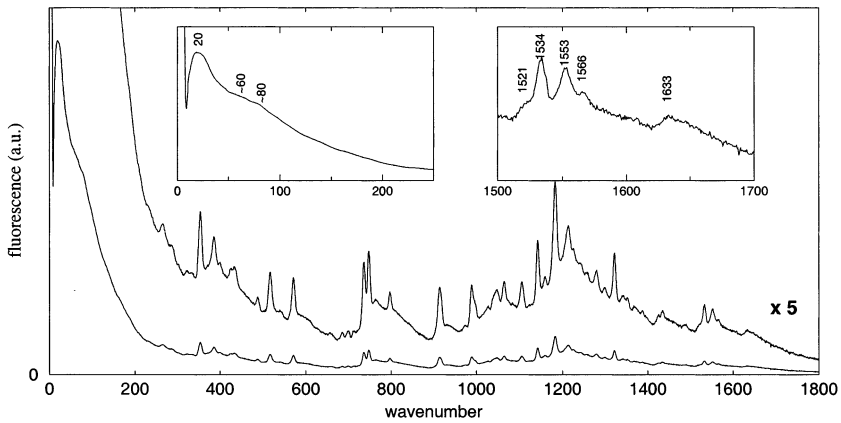

FIGURE 7: Line-narrowed emission spectrum of CP47 at 4 K. The spectrum is the average of the spectra excited at 692.4, 692.8, and 694.4 nm, converted to the wavenumber scale and plotted as the difference with the excitation wavenumber. Insets show the phonon wing region and the region of the C═C and the 13^1 C═O stretch modes.

Table 2: Comparison between the Vibrational Frequencies as Obtained for the Emission of CP47 at 4 K and Literature Values for the Other Subcomplexes of the PSII Core, CP43 (*34*), and the Reaction Center (*16*)[a]

RC	CP43	CP47	RC	CP43	CP47	RC	CP43	CP47
19	24	20	678 w	681 w		1178 s	1188 s	1184 s
37	52	~60		691 w	686 w	1200 w		
~80	~86	~80	695 w	703 w	700 w	1211 m	1221 m	1214 m
157 w	120 w		711 m		713 w	1223 m	1231* m	1226 w
179 m	175 m		725 w	725 w		1242 m	1238 w	1244 w
197 m	200 w		748 s	742 s	737 s	1256 w	1263 w	1258 w
250 s	254 m		756 m	755 s	748 s	1270 w	1273 w	
	267 m	266 m	769 w	769 w	766 w	1282 w	1286 m	1280 m
	284 w	289 w	786 w			1296 w	1308 w	1300 w
302 w	305 w	303 w	802 w	801 w	798 m	1325 s	1330 s	1322 s
		324 w	846 w	836 w		1343 w		1342 w
344 s	349 s	337 w	860 w			1354 w	1354 m	1353 w
361 s		355 s	906 m	902 w		1374 w	1373 w	1371 w
384 s	378 m	387 s	918 s	917 s	916 s	1389 w	1392 w	1388 w
	395 m	401 w	962 w	945 w	974 w		1422 w	1425 w
	415* w		987 s	987 s	990 s	1437 m	1438 m	1436 w
	424 w	426 w	1010 w	1000 w	1000 w	1453 w	1456 w	
430 m	431 w	434 m	1025 w	1019 w	1028 w		1470 w	
	448 m		1042 m	1041 m	1040 w	1491 w	1490 w	1490 w
474 m	471 m		1051 w	1054 w	1049 w		1527 w	1520 w
489 w	487 w	489 m	1067 w	1068 m	1065 m	1536 s	1537 s	1534 s
499 m	500 m		1073 w		1076 w	1555 s	1556 s	1553 s
518 s	525 s	518 s	1089 w					1566 w
542 w	544* w	543 w	1110 m	1110 w	1107 m	1587 w	1587 w	
560 w	561* w		1123 w	1117 m		1612 w	1610 w	
570 m	576 m	571 s		1133 w			1628* w	1633 m
	591 w		1141 s	1146 s	1143 s	1660 w	1658* w	
612 m	606 w		1159 w	1160 w	1160 w	1669 w	1671 w	
658 w	648 w	662 w	1169 w	1166 w				

[a] CP43 modes denoted with * are only observed with excitation between 679 and 682 nm. The relative intensities of the vibronic features are denoted with s (strong), m (medium), and w (weak).

complicated mixture of similarities and differences among the three subcomplexes of the PSII core.

The emitter upon red-most excitation is naturally assigned to the 690 nm pigment. Hydrogen bonding of the 13^1 keto group to a protein ligand is known to induce a red shift of the Chl Q_y 0−0 transition. Krawczyk (*37*) obtained an empirical relation: $\Delta\lambda = 0.23\ (1686.7 - \nu_{C=O})$. Using the value of 1633 cm^{-1} then implies a red shift of 12 nm. In the bacterial LH1 and LH2 complexes, the break of a hydrogen bond was shown to cause a large blue shift of the B850 bacteriochlorophyll ring (*38*−*40*).

Upon scanning the excitation wavelength more to the blue (<692 nm), the vibrational finestructure changed in the region of the C═C and 13^1 C═O stretch modes. The major change is a decreased intensity of the mode at ~1633 cm^{-1} and an appearance of a mode at ~1664 cm^{-1} (see Figure 8), indicating that at this excitation wavelength at least part of the 4 K fluorescence originates from a different Chl (part of the 683 nm state) with weaker hydrogen bonding. Comparable observations were made for the CP43 complex (*34*): Upon far-red excitation (>684 nm) the 13^1 C═O stretch frequency is observed at 1671 cm^{-1}, whereas upon excitation at 682−683 nm this stretch is also observed at 1658 cm^{-1}. In the former case a broad excitonic band in CP43 is excited, while at about 682 nm a narrow band is found in the CP43 absorption spectrum (presumably corresponding to a single Chl), suggesting that also in CP43 strong hydrogen bonding of a single Chl introduces a red-shifted state.

We showed that, for all excitation wavelengths, most emitting Chls are five-coordinated (with a minor contribution of six-coordinated Chls) and hydrogen bonded to the protein (though the observed bond strength does depend on the

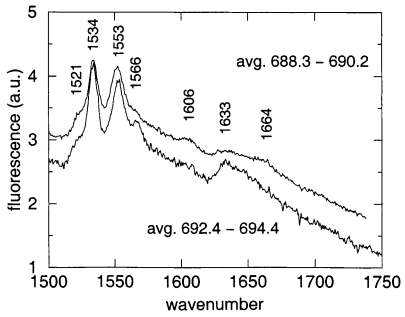

FIGURE 8: Line-narrowed emission spectrum of CP47 at 4 K in the region of the C═C and the 13^1 C═O stretch modes. The upper spectrum is the average of spectra excited at 688.3, 689.2, and 690.2 nm. The lower spectrum is the average of spectra excited at 692.4, 692.8, and 694.4 nm.

excitation wavelength). In a resonance Raman study (*41*) sensitive to all Chls in the CP47 complex, Raman shifts observed at 1563 and 1617 cm^{-1} were claimed to reflect the C═C stretches of all Chls being five-coordinated. A Raman shift at ~1670 cm^{-1} was assigned to part of the Chls being hydrogen bonded to the protein. Probably the spectral features of a minor amount of six-coordinated Chls and of a single Chl having a strong hydrogen bond have not been resolved in this Raman study.

Stark Spectroscopy. The Stark spectrum is the difference absorption spectrum observed upon applying an external electrostatic field. A highly concentrated sample is needed to achieve a considerable OD over the small distance (~0.1 mm) between the electrodes. As a result, some aggregation of the CP47 complexes appeared unavoidable. This can be inferred from the absorption spectrum in the Stark cell, shown in Figure 9 (top, squares). This spectrum exhibits slightly more absorption on the blue side of the Q_y transition than the absorption spectrum in Figure 1. However, the shoulder at 683 nm and the tailing of the spectrum toward the red are obvious.

The Stark spectrum is shown in Figure 9 (bottom, squares). The spectrum exhibits a broad minimum around 665 nm, a distinct minimum at 673.5 nm, a complicated structure around 680 nm, and a distinct maximum at 684 nm tailing up to 700 nm. The spectrum resembles the first derivative of the absorption (not shown); hence, a change in polarizability (Tr($\Delta\alpha$)) rather than a change in permanent dipole between the ground and excited states ($\Delta\mu$) dominates the Stark spectrum. The Stark spectrum bears an overall resemblance to the Stark spectrum of CP43, the other PSII core antenna protein (*34*).

Six Gaussians were needed for a simultaneous fit of the absorption and Stark spectra (see Figure 9, top). Despite some aggregation of the CP47 complexes in the Stark experiment, the positions of the Gaussians in Figure 9 are within 1 nm of the positions shown in Figure 3, and the relative amplitudes are only slightly different from those in Figure 3. The fitted absorption and Stark spectra are represented by solid lines, the fitted first derivative contribution to the Stark spectrum by dotted lines and fitted second derivative contribution by dashed lines. The resulting Tr($\Delta\alpha$) and $\Delta\mu$ values for each band are listed in Table 3. The Tr($\Delta\alpha$) values range (going from blue to red) from 20 to 60 $Å^3$ f^{-2}, and the value of $\Delta\mu$ is 0.3−0.4 D f^{-1} for all bands, except the most

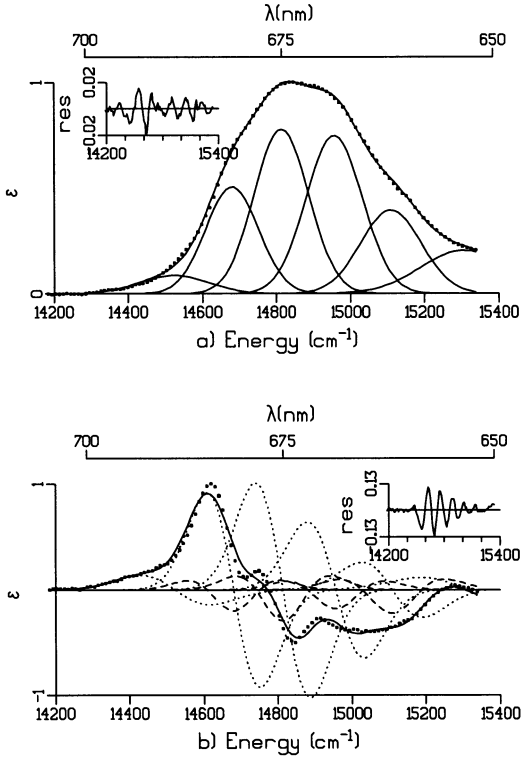

FIGURE 9: Simultaneously recorded absorption (top) and Stark (bottom) spectra of CP47 at 77 K. Data points are indicated by squares. Also shown is a simultaneous fit of both spectra (solid lines), with the absorption as a sum of six Gaussians (solid lines) and the Stark spectrum as a sum of first (dotted lines) and second (dashed lines) derivatives of the same Gaussians. The insets show the residuals.

Table 3: Values of the Spectral Position, Difference in Permanent Dipole Moment ($\Delta\mu$), and Difference in Polarizability (Tr($\Delta\alpha$)), Obtained from the Simultaneous Fit of Absorption and Stark Spectra of CP47 at 77 K[a]

pos (±1 nm)	*Tr*($\Delta\alpha$) (±10 $Å^3$ f^{-2})	$\Delta\mu$ (±0.1 D f^{-1})
653	27	0.0
662	22	0.4
669	27	0.3
675	39	0.3
681	53	0.3
689	61	0.0

[a] See Also Figure 9.

blue and most red transition which have a $\Delta\mu$ value equal to zero.

The values for $\Delta\mu$ are lower than those for monomeric (0.9−1.0 D f^{-1}) and dimeric (5 D f^{-1}) Chl (*42*) and are close to those obtained in CP43. As in CP43, this may be explained by the idea that the absorption of CP47 originates from a set of excitonic transitions, in which the contributing dipoles have opposing orientations (antiparallel).

The values for Tr($\Delta\alpha$) are much higher than obtained in CP43 (5−6 $Å^3$ f^{-2}, see ref *34*), and are between values obtained for monomeric (1.5−4 $Å^3$ f^{-2}) and dimeric (90 $Å^3$ f^{-2}) Chl (*42*). This is in line with the larger extend of excitonic coupling in CP47 than in CP43 (*10*).

DISCUSSION

In this paper we have provided new spectroscopic information of the red-most states of the Chls of CP47. The lowest

state absorbs at 690 nm, has an oscillator strength of approximately one Chl and is oriented at large angles with the plane of the thylakoid membrane, thereby supporting the original conclusion by Van Dorssen et al. (*4*, *5*). In the Stark response, this state shows a larger difference in polarizability (between ground and excited state) but a smaller difference dipole moment compared to that of monomer Chl *a*. A mode at ~1633 cm^{-1} in the FLN spectrum can most likely be assigned to an extremely downshifted stretch frequency of the Chl 13^1 keto group, suggesting that this group is strongly hydrogen bonded to a protein ligand. Thus, the red shift of the Q_y (0−0) transition of this "red" Chl is very likely not caused by excitonic interactions, but must probably to a large extent be explained by the strong hydrogen bond of the Chl 13^1 keto group (see also ref *37*). This conclusion is in agreement with our time-resolved analysis (*10*) and with the absence of a prominent contribution to the circular dichroism (CD) spectrum (*17*). We have found no evidence for a coupling of the 690 nm state to a state at 687 nm, as suggested by Chang et al. (*11*). We note that to invoke such a weakly coupled dimer (coupling much smaller than the disorder) is perhaps not realistic, and certainly does not explain the total red shift.

The second important red state absorbs maximally at 683 nm, has an oscillator strength of approximately three Chls, and is oriented at small angles with the plane of the thylakoid membrane. In the Stark response, this state shows a similar difference in polarizability but a larger difference in dipole moment compared to the 690 nm state. From site-selective polarized triplet spectra, an excitonic origin for the 683 nm state was found (coupling to higher energy states), in agreement with the CD characteristics (*17*). At least part of the 683 nm state contributes to the 4 K emission, as can be concluded from the changing anisotropy of the emission over the emission band upon excitation around 683 nm, versus a constant high value after excitation more to the red. The stretch frequency of the 13^1 keto group of this emitting 683 nm Chl (from the line-narrowing data there is no indication for several emitting 683 nm Chls) is much less downshifted, suggesting that this group of Chls is much less strongly hydrogen bonded to the protein (than the 690 nm pigment). The other part of the 683 nm state, transferring to the 690 nm pigment, probably corresponds to the 684 nm state in the study by Chang et al. (*11*).

The conclusion that at least two emitters exist in CP47 is consistent with earlier observations. In a transient absorption study at 77 K, only part of a species with its bleaching/stimulated emission centered at 683 nm relaxes to the 690 nm pigment, resulting in a broad and nonsymmetric difference spectrum (*10*). Also, the large width of the nonselectively excited 4 K fluorescence (fwhm 12.5 nm) supports this idea (*12*). The presence of at least two spectrally different emitters is most easily explained by the idea that, due to inhomogeneous broadening of the absorption lines, in some CP47 complexes "683 nm" Chls must exist that are in fact redder than the 690 nm pigment. Furthermore, one cannot be sure that at 4 K all excitations are able to reach the lowest state, and therefore contributions from states higher than the 690 nm pigment (the 683 nm state) can contribute more to the fluorescence than expected from a thermally equilibrated excitation distribution. Also CP43 possesses two closely spaced states that are essentially noninteracting (*34*, *43*).

We note again that two species peaking at 684 and 686 nm (the former bearing half the amplitude of the latter) are present in time-resolved T−S spectra (*12*). It was suggested from the short triplet state lifetime of the 686 nm species that at least one Chl is six-coordinated and hydrogen bonded to the protein. How can we relate these species to the 683 and 690 nm states identified here?

Our line-narrowing study indicates that the 690 nm state cannot correspond to the six-coordinated 686 nm species: For all excitation wavelengths, most emitting Chls are five-coordinated (with only a minor contribution of six-coordinated Chls). A 690 nm band is absent in our site-selective T−S spectra, most likely because it is permanently bleached due to the high excitation powers. At the moment we can only speculate why a 690 nm band is not observed in the time-resolved T−S spectra (*12*). If the 690 nm state is part of an excitonic manifold, the changing Chl-Chl interactions upon triplet formation might cause a bleach at ~685 nm. If not, one has to consider a special decay channel of the 690 nm triplet, such as the preferential triplet transfer to β-carotene (*12*). In addition triplet transfer from the 690 nm Chl to the 683 nm Chl may occur on a submicrosecond time scale. Following the assumption of a nonobserved 690 nm triplet, we suggest that the "684 nm" and "686 nm" species reflect the transferring and nontransferring 683 nm states identified earlier. In this assumption, a triplet might be present on the transferring 683 nm state, either because not all of these states are actually transferring (due to inhomogeneous broadening), or because of the possible triplet−triplet transfer from the 690 nm state.

In the following we will attempt to link all the 683 and 690 nm states to the Chls identified in the recent structure (*6*). In an earlier paper, we proposed two pairs of Chls with strong pairwise interactions (the Chl pairs 39−42 and 35−48, nomenclature as in ref *6*, see also Figure 10) as candidates for the 683 nm states (*10*). Repeating the exciton calculations as in our previous report (*10*), but based on the heme planes as specified in a later interpretation of the same X-ray data (*7*), suggests a larger red shift of a third pair of Chls (41−45), so that also this pair might contribute to the 683 nm states. However, the total oscillator strength of the 683 nm corresponds to approximately three Chls, which (because most oscillator strength of all these dimers is in the low-energy transitions) implies that at most two "dimers" can contribute to the 683 nm state. In the later interpretation of the X-ray data by Vasil'ev et al. (*7*), one of the two additional Chls present in CP47 (no. 36, nomenclature of ref *7*) is close to His-114 and serves as the most likely candidate for the 690 nm pigment (*8*). In Figure 10, we denoted this Chl as no. 114. Although this Chl is very close (~8 Å) to Chl 46, our experiments suggest that the 690 nm pigment is not strongly coupled to any other Chl. However, for an orientation of the Chl 114 dipole out of the membrane plane (to obtain the correct LD sign) and an orientation of the Chl 46 dipole in the membrane plane, the mutual orientation factor κ^2 is small and the resulting coupling weak. Moreover, an orientation of the Chl 46 dipole out of the membrane plane does result in a strong coupling but produces a blue rather than a red shift.

The energy transfer that takes place between the 683 and 690 nm states is now considered. We tried to rotate the dipole of Chl 114 in such a way that (i) it is making an angle to

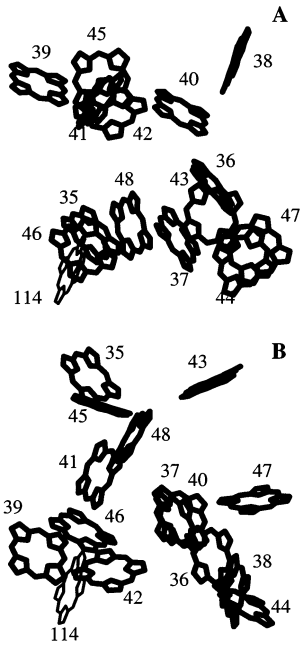

FIGURE 10: (A) Structure of CP47 looking along the plane of the membrane. Luminal side is at the top; stromal side is at the bottom. (B) Structure looking from the luminal side. The RC is on the right-hand side of CP47 in both pictures. Chls 35−48 have been taken from ref *6*. The Chl drawn with thinner lines (labeled 114) is the additional Chl close to Histidine-114 that is present in a further analysis of the same X-ray data (*7*), and that is the prime candidate for the 690 nm pigment (*8*).

the membrane plane larger than 35° (to obtain the correct LD sign), (ii) the transfer from both Chls of one of the three Chl pairs to the 690 nm pigment becomes nonexistent (i.e., the orientation factor κ^2 becomes near-zero), and (iii) the transfer from at least one of the other two dipoles to the 690 nm pigment is in the order of 20 ps (using the Förster equation, see ref *10*).

We conclude that such an orientation of Chl 114 exists (starting with an orientation in the membrane plane, the dipole should be rotated ∼75° within the heme plane, in such a way that it is making an angle of ∼60° with the NB−ND axis specified by Vasil'ev et al. (*7*)), and the resulting nontransferring state is the Chl pair 35−48. In this calculation, both other dimers can still account for the transferring 683 nm state. We note that so far we considered only downhill energy transfer (to the 690 nm pigment), but at 77 K (as in our pump−probe experiment, see ref *10*) also transfer to isoenergetic states or states slightly higher in energy should be considered. In our calculations, given the dipole realizations in the membrane plane, the Chl 35−48 dimer is indeed isolated from the 39−42 dimer, but does transfer to the 41−45 dimer on the time scale of a few (tens of) picoseconds. Of course, this depends on the orientations of the pigments, a large rotation (tens of degrees) can change this picture. However, following our assumptions, we suggest that the Chl 41−45 pair is in fact at higher energy (∼6 nm), making the Chl 35−48 sufficiently low in energy to avoid back transfer. We thus suggest that the Chl pair 35−48 is the nontransferring 683 nm state observed in the 77 K time-resolved pump−probe spectra, while the Chl pair 39−42 is the 683 nm state transferring in about 20 ps to Chl 114 that absorbs at 690 nm, but we stress that a final assignment is only possible when knowing the exact orientations of the transition dipoles.

At room temperature there is no trap for the excitation energy, and the excitation distribution is given by a Boltzmann distribution over all Chls. The 690 nm pigment (Chl 114) is not close to Chl 43, the Chl closest to the reaction center. Therefore, the presence of the red 690 nm pigment will slow down rather than speed up the energy transfer to the reaction center, but this effect will most likely be small.

ACKNOWLEDGMENT

We thank Henny van Roon for the expert preparation of the CP47 particles.

REFERENCES

1. Van Grondelle, R., Dekker, J. P., Gillbro, T., and Sundström, V. (1994) *Biochim. Biophys. Acta 1187*, 1−65.
2. Diner, B. A., and Babcock, G. T. (1996) in *Oxygenic Photosynthesis: The Light Reactions* (Ort, D. R., and Yocum, C. F., Eds.) pp 213−247, Kluwer Academic Publishers, Dordrecht, The Netherlands.
3. Nugent, J. H. A. (1996) *Eur. J. Biochem. 237*, 519−531.
4. Van Dorssen, R. J., Breton, J., Plijter, J. J., Satoh, K., Van Gorkom, H. J., and Amesz, J. (1987) *Biochim. Biophys. Acta 893*, 267−274.
5. Van Dorssen, R. J., Plijter, J. J., Dekker, J. P., Den Ouden, A., Amesz, J., and Van Gorkom, H. J. (1987) *Biochim. Biophys. Acta 890*, 134−143.
6. Zouni, A., Witt, H.-T., Kern, J., Fromme, P., Krauss, N., Saenger, W., and Orth, P. (2001) *Nature 409*, 739−743.
7. Vasil'ev, S., Orth, P., Zouni, A., Owens, T. G., and Bruce, D. (2001) *Proc. Natl. Acad. Sci. U.S.A.* 98, 8602−8607.
8. Shen, G., and Vermaas, W. F. J. (1994) *Biochemistry 33*, 7379−7388.
9. Shen, J. R., and Kamiya, N. (2000) *Biochemistry 39*, 14739−14744.
10. De Weerd, F. L., Van Stokkum, I. H. M., Van Amerongen, H., Dekker, J. P., and Van Grondelle, R. (2002) *Biophys. J. 82*, 1586−1597.
11. Chang, H.-C., Jankowiak, R., Yocum, C. F., Picorel, R., Alfonso, M., Seibert, M., and Small, G. J. (1994) *J. Phys. Chem. 98*, 7717−7724.
12. Groot, M.-L., Peterman, E. J. G., Van Stokkum, I. H. M., Dekker, J. P., and Van Grondelle, R. (1995) *Biophys. J. 68*, 281−290.
13. Dekker, J. P., Bowlby, N. R., and Yocum, C. F. (1989) *FEBS Lett. 254*, 150−154.
14. Otte, S. C. M., Van der Vos, R., and Van Gorkom, H. J. (1992) *J. Photochem. Photobiol. B: Biol. 15*, 5−14.
15. Visschers, R. W., Chang, M. C., Van Mourik, F., Parkes-Loach, P. S., Heller, B. A., Loach, P. A., and Van Grondelle, R. (1991) *Biochemistry 30*, 5734−5742.
16. Peterman, E. J. G, Van Amerongen, H., Van Grondelle, R., and Dekker, J. P. (1998) *Proc. Natl. Acad. Sci. U.S.A.* 95, 6128−6133.
17. Kwa, S. L. S., Völker, S., Tilly, N. T., Van Grondelle, R., and Dekker, J. P. (1994) *Photochem. Photobiol. 59*, 219−228.
18. Beekman, L. M. P., Frese R. N., Fowler G. J. S., Picorel, R., Cogdell R. J., Van Stokkum, I. H. M., Hunter, C. N., and Van Grondelle, R. (1997) *J. Phys. Chem. B 101*, 7293−7301.
19. Liptay, W. (1974) in *Excited States Vol. I* (Lim, C. E., Ed.) pp 128−190, Academic Press, New York.
20. Bublitz, G. U., and Boxer, S. G. (1997) *Annu. Rev. Phys. Chem. 48*, 213−242.
21. Beekman, L. M. P., Steffen, M., Van Stokkum, I. H. M., Olsen, J. D., Hunter C. N., Boxer, S. G., and Van Grondelle, R. (1997) *J. Phys. Chem. B 101*, 7284−7292.
22. Gülen, D., Van Grondelle, R., and Van Amerongen, H. (1997) *J. Phys. Chem. B 101*, 7256−7261.
23. Gradinaru, C. C., Özdemir, S., Gülen, D., Van Stokkum, I. H. M., Van Grondelle, R., and Van Amerongen, H. (1998) *Biophys. J. 75*, 3064−3077.
24. Van Amerongen, H., and Van Grondelle, R. (2001) *J. Phys. Chem. B 105*, 604−617.

25. Kwa, S. L. S., Newell, W. R., Van Grondelle, R., and Dekker, J. P. (1992) *Biochim. Biophys. Acta 1099*, 193−202.
26. Germano, M., Shkuropatov, A. Y., Permentier, H., De Wijn, R., Hoff, A. J., Shuvalov, V. A., and Van Gorkom, H. J. (2001) *Biochemistry 40*, 11472−11482.
27. Den Hartog, F. T. H., Dekker, J. P., Van Grondelle, R., and Völker, S. (1998) *J. Phys. Chem. B 102*, 11007−11016.
28. Van Amerongen, H., Vasmel, H., and Van Grondelle, R. (1988) *Biophys. J. 54*, 65−76.
29. Ruban, A. V., Calkoen, F., Kwa, S. L. S., Van Grondelle, R., Horton, P., and Dekker, J. P. (1997) *Biochim. Biophys. Acta 1321*, 61−70.
30. Kwa, S. L. S., Eijckelhoff, C., Van Grondelle, R., and Dekker, J. P. (1994) *J. Phys. Chem. 98*, 7702−7711.
31. Fujiwara, M., and Tasumi, M. (1986) *J. Phys. Chem. 90*, 250−255.
32. Fujiwara, M., and Tasumi, M. (1986) *J. Phys. Chem. 90*, 5646−5650.
33. Lutz, M., and Robert. B. (1988) in *Biological Application of Raman Spectroscopy* (Spiro, T. G., Ed.) pp 347−411, Wiley, New York.
34. Groot, M.-L., Frese, R. N., De Weerd, F. L., Bromek, K., Pettersson, Å., Peterman, E. J. G., Van Stokkum, I. H. M., Van Grondelle, R., and Dekker, J. P. (1999) *Biophys. J. 77*, 3328−3340.
35. Peterman, E. J. G, Pullerits, T., Van Grondelle, R., and Van Amerongen, H. (1997) *J. Phys. Chem. B 101*, 4448−4457.
36. Peterman, E. J. G., Wenk, S.-O., Pullerits, T., Pålsson, L.-O., Van Grondelle, R., Dekker, J. P., Rögner, M., and Van Amerongen, H. (1998) *Biophys. J. 75*, 389−398.
37. Krawczyk, S. (1989) *Biochim. Biophys. Acta 976*, 140−149.
38. Fowler, G. J. S., Visschers, R. W., Grief, G. G., Van Grondelle, R., and Hunter, C. N. (1992) *Nature 355*, 848−850.
39. Olsen, J. D., Sturgis, J. N., Westerhuis, W. H. J., Fowler, G. J. S., Hunter, C. N., and Robert, B. (1997) *Biochemistry 36*, 12625−12632.
40. Lapouge, K., Näveke, A., Gall, A., Ivancich, A., Seguin, J., Scheer, H., Sturgis, J. N., Mattioli, T. A., and Robert, B. (1999) *Biochemistry 38*, 11115−11121.
41. De Paula, J. C., Liefshitz, A., Hinsley, S., Lin, W., Chopra, V., Long, K., Williams, S. A., Betts, S., and Yocum, C. F. (1994) *Biochemistry 33*, 1455−1466.
42. Krawczyk, S. (1991) *Biochim. Biophys. Acta 1056*, 64−70.
43. Jankowiak, R., Zazubovich, V., Rätsep, M., Matsuzaki, S., Alfonso, M., Picorel, R., Seibert, M., and Small, G. J. (2000) *J. Phys. Chem. B 104*, 11805−11815.

BI0261948